Using ENVISAT ASAR Global Mode Data for Surface Soil Moisture Retrieval Over Oklahoma, USA

Carsten Pathe, Wolfgang Wagner, *Senior Member, IEEE*, Daniel Sabel, Marcela Doubkova, and Jeffrey B. Basara

***Abstract*—The advanced synthetic aperture radar (ASAR) onboard of the satellite ENVISAT can be operated in global monitoring (GM) mode. ASAR GM mode has delivered the first global multiyear C-band backscatter data set in HH polarization at a spatial resolution of 1 km. This paper investigates if ASAR GM can be used for retrieving soil moisture using a change detection approach over large regions. A method previously developed for the European Remote Sensing (ERS) scatterometer is adapted for use with ASAR GM and tested over Oklahoma, USA. The ASAR-GM-derived relative soil moisture index is compared to 50-km ERS soil moisture data and pointlike *in situ* measurements from the Oklahoma MESONET. Even though the scale gap from ASAR GM to the *in situ* measurements is less pronounced than in the case of the ERS scatterometer, the correlation for ASAR against the *in situ* measurements is, in general, somewhat weaker than for the ERS scatterometer. The analysis suggests that this is mainly due to the much higher noise level of ASAR GM compared to the ERS scatterometer. Therefore, some spatial averaging to 3–10 km is recommended to reduce the noise of the ASAR GM soil moisture images. Nevertheless, the study demonstrates that ASAR GM allows resolving spatial details in the soil moisture patterns not observable in the ERS scatterometer measurements while still retaining the basic capability of the ERS scatterometer to capture temporal trends over large areas.**

***Index Terms*—Change detection, ScanSAR, scatterometer, soil moisture, synthetic aperture radar (SAR).**

I. Introduction

SOIL MOISTURE is a key element in the global cycles of water, energy, and carbon. Knowledge on the status of the soil moisture content is therefore essential for hydrology, meteorology, climatology, agronomy, and many other earth sciences. Soil moisture should also be regarded as an important socioeconomic factor. It is expected that two thirds of the world's population will experience a shortage of fresh water due to population growth and the effects of climate change in the year 2025 [1]. To alleviate some of the ensuing societal problems, advances in data collection and hydrologic modeling are required for a more effective management of fresh water supply for people and food production, predicting extreme events like droughts and floods, and protecting ecosystems. Unfortunately, in many regions where water resources and the water environment are under threat, measurement networks are not well developed and, in some cases, even undergoing further cutbacks [2]. According to [3], runoff measurement reports from African countries declined dramatically during the 1990s.

Soil moisture can be measured accurately in the field using *in situ* measurement techniques [4]. However, there are only few soil moisture networks worldwide [5]. Alternatively, soil moisture can be measured using remote sensing at different temporal and spatial scales [6]. Microwave remote sensing instruments operated at frequencies below the relaxation frequency of water molecules (9 GHz near 0 °C and 17 GHz at 20 °C) hold the largest potential for the retrieval of soil moisture because of the large dielectric contrast between dry and wet soil at these frequencies. Already in the 1970s, radiometer and scatterometer measurements acquired from board of Skylab, which is the first space station of the U.S., demonstrated the sensitivity of active and passive microwave measurements to soil moisture [7]. However, the measurements are also affected by vegetation, surface roughness, and other land surface parameters. Therefore, the sensor and the retrieval method must be carefully chosen in order to achieve accurate soil moisture retrievals.

In recent years, significant progress has been made in the use of coarse-resolution (25–50 km) radiometer and scatterometer systems for soil moisture retrieval [8]. There are now several soil moisture products derived from low frequency (< 10 GHz) radiometer measurements such as provided by the Advanced Microwave Scanning Radiometer for the Earth Observing System [9]–[11] and from C-band (5.3 GHz) scatterometer measurements [12]–[14]. Several of these soil moisture products have been shared with the scientific community, and the first product validation and intercomparison studies using *in situ* soil moisture measurements [8], model simulations [15], and novel data assimilation approaches [16] have been carried out. These studies showed that the accuracy of the retrieved soil moisture data depends strongly on the employed retrieval technique, while sensor specifications appear to be less important, i.e., good and comparable retrievals can be achieved from

Manuscript received February 1, 2008; revised May 19, 2008 and July 15, 2008. Current version published January 28, 2009. This work was supported in part by the European Space Agency (ESA) through the SHARE Project, by the Austrian Science Fund (FWF) through Project MISAR (P16515-N10), and by the Austrian Research Promotion Agency (FFG) through Projects ENVISAT-AO 356 and EO-NatHaz (ALR-OEWP-CO-413/07).

C. Pathe, W. Wagner, D. Sabel, and M. Doubkova are with the Institute of Photogrammetry and Remote Sensing, Vienna University of Technology, 1040 Vienna, Austria (e-mail: radar@ipf.tuwien.ac.at; cp@ipf.tuwien.ac.at; ww@ipf.tuwien.ac.at; ds@ipf.tuwien.ac.at; mdo@ipf.tuwien.ac.at).

J. B. Basara is with the Oklahoma Climatological Survey, The University of Oklahoma, Norman, OK 73072-7305 USA (e-mail: jbasara@ou.edu).

Digital Object Identifier 10.1109/TGRS.2008.2004711

both active and passive measurements below about 10 GHz. Nevertheless, it is expected that the Soil Moisture and Ocean Salinity (SMOS) mission, which is the first satellite dedicated to the retrieval of soil moisture over land [17], will provide more accurate soil moisture data than the existing sensors. SMOS uses an interferometric radiometer operated in L-band to minimize the impacts of vegetation and surface roughness on the signal.

The major disadvantage of spaceborne microwave radiometers and scatterometers is their low spatial resolution (25–50 km). A higher spatial resolution can only be achieved by active microwave instruments (AMIs) that provide subantenna footprint resolution by means of range and Doppler discrimination [18]. The concept of range and Doppler discrimination is employed by side-looking synthetic aperture radars (SARs) designed to acquire high resolution backscatter images. It can also be employed by conically scanning radar instruments, such as in the case of the Hydrosphere State mission [19], which was cancelled by NASA in 2005 but recently revived as the Soil Moisture Active Passive mission.

As pointed out by Kerr [20], the most adverse characteristic of synthetic aperture techniques is linked to the coherent nature of the signal due to the system design itself. Due to the coherent measurement process, the superposition of waves reflected by scatterers at the Earth's surfaces leads to a grainlike appearance of SAR images ("speckle") and a high sensitivity of the measurements to the geometric arrangement of the scatterers [21]. As a result, SAR measurements are very sensitive to the roughness of the soil surface and the geometry of the vegetation. Research has shown that the influences of surface roughness and vegetation on the backscattered signal are comparable or larger than the influence of soil moisture [22], [23]. Therefore, spatial patterns observed in SAR images are primarily related to the spatial patterns of surface roughness and vegetation, and only to a lesser extent to spatial soil moisture variations. Kerr [20] suggests that, because of these inherent difficulties, SAR systems have neither been used in a standard and routine fashion nor have they resulted in any useful maps of absolute soil moisture.

Despite the important influence of roughness and vegetation, many studies have shown that soil moisture changes can be tracked by SAR image time series using change detection approaches [24], [25]. In change detection, a reference image is subtracted from each individual SAR image in an attempt to correct for roughness and vegetation effects specific to each pixel of an image. Unfortunately, spaceborne SAR systems are generally not designed to obtain repetitive and continuous coverage, which has hampered the applicability of change detection approaches [26]. The problem is that SAR image modes have a high power consumption which limits the operation time per orbit (duty cycle). For example, the German satellite TerraSAR-X can acquire X-band SAR images with a resolution of up to 1 m, but it can only be switched on for about 20% of the time of each orbit [27]. Therefore, long time series with 100 or more SAR images covering the same area are generally not available.

Coverage can be improved by increasing the duty cycle at the expense of the spatial and/or radiometric resolution and by using ScanSAR technology to image a wide swath. The ScanSAR technique is based on electronic beam steering and sharing of the operational time of the sensor between adjacent subswaths [28]. This leads to a decrease in azimuth resolution and an increase of the incidence angle range of each processed ScanSAR scene. Most of the spaceborne SAR instruments onboard of the latest generation of radar satellites utilize ScanSAR technology to cover swath widths on the order of 200 to 500 km. However, only the advanced SAR (ASAR) onboard of the European satellite ENVISAT has a ScanSAR mode that can potentially be operated continuously. It is called the global monitoring (GM) mode, has a swath width of 400 km, and has been operated as ASAR background mission over land since December 2004. Consequently, most land surface areas have been covered more than 100 times with ASAR GM, some high-latitude areas even more than 400 times (Fig. 1).

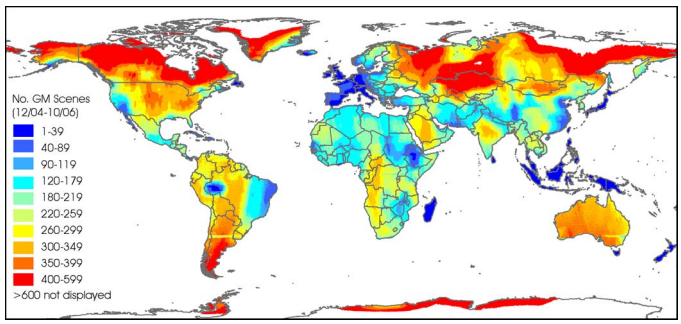

Fig. 1. Number of ASAR GM mode acquisitions in the period December 2004 to October 2007.

In several aspects, ASAR GM mode is comparable to the scatterometer mode of the AMI onboard the European Remote Sensing (ERS) satellites ERS-1 and ERS-2. Both ASAR GM and the ERS scatterometer have delivered the first global multiyear C-band backscatter data sets at their respective spatial resolution, i.e., 50 km for the ERS scatterometer and 1 km for ASAR GM. Furthermore, the global coverage of the ERS scatterometer resembles in many important features (e.g., poor coverage of Europe) to the one of ASAR GM because the AMI scatterometer mode cannot be operated in parallel to the AMI SAR modes [29]. Important differences are that the AMI scatterometer makes three independent backscatter measurements at vertical polarization with a high radiometric accuracy (< 0.2 dB) from different viewing directions using its three antennas, while ASAR GM acquires only one backscatter measurement usually at horizontal polarization with a radiometric accuracy of about 1.2 dB.

Considering the technical similarities of the ERS scatterometer and ASAR GM, and the successful application of change detection approaches to scatterometer and SAR time series demonstrated in many studies [26], it is hypothesized that ASAR GM can be used for monitoring surface soil moisture using a change detection approach. To verify this hypothesis, a change detection method developed for the ERS scatterometer [30]–[32] is adapted for use with ASAR GM time series. The retrieved soil moisture values are compared to *in situ* soil moisture observations and scatterometer retrieved soil moisture data. Oklahoma, USA, was chosen as study area because of the

good ASAR GM coverage and the availability of *in situ* soil moisture observations from the Oklahoma MESONET [33].

II. Theory

SARs radiate short coherent microwave pulses toward the Earth's surface and record the phase and amplitude of the backscattered signals. The amplitude of the complex signal depends on the technical configuration of the SAR sensor (frequency, polarization, and look angle), as well as the geometric and dielectric properties of the Earth's surface [34], [35]. In theory, an exact solution could be obtained by solving Maxwell's equation. However, given the complex shapes of natural soil surfaces and vegetation canopies, an analytical solution is not feasible. Only approximate solutions that are critically dependent on the validity of the underlying assumptions can be derived analytically.

In recent years, the applicability of theoretical models for describing scattering by natural soil surfaces and vegetation has increasingly been questioned. In the case of bare soil backscatter models, the problems appear to be mainly related to the characterization of the roughness of natural soil surfaces [36]. As a result, many experimental studies did not find a satisfactory match between modeled and measured bare soil backscatter [37]–[39]. In the case of vegetation scattering models, ground-based and airborne measurements with radar instruments capable of resolving the vertical backscattering profile of vegetation canopies revealed that the penetration of the microwaves into the vegetation canopy has often been underestimated by the models [40], [41].

The shortcomings of bare soil and vegetation backscatter models mainly affect our capability to model the absolute backscatter level in terms of physical soil and vegetation parameters, such as the rms height of soil surface and the vegetation water content. Change detection methods try to circumvent these difficulties by solely interpreting backscatter changes, without attempting to explain the absolute backscatter level. The change detection model developed for the ERS scatterometer by [30]–[32] describes backscatter expressed in decibels in terms of empirical backscatter parameters and the relative surface soil moisture content m_s

$$\sigma^0(\theta,t) = \sigma^0_{\rm dry}(\theta,t) + S(t)m_s(t) \tag{1}$$

where θ is the local incidence angle, t is the time, $\sigma^0_{\rm dry}$ is the backscattering coefficient observed under completely dry soil conditions in decibels, and S is the sensitivity of the backscattering coefficient σ^0 to changes in soil moisture in decibels. The relative soil moisture content m_s ranges from zero in dry soil to unity (or 100%) in a completely saturated soil. It is equivalent to the degree of saturation, which is the volume of water present in the soil relative to the volume of pores [42]. Note that in (1), S is constant over the entire incidence angle range of the ERS scatterometer from 18° to 59°.

The backscatter model parameters $\sigma^0_{\rm dry}$ and S depend on surface roughness and vegetation conditions and vary, in general, strongly in space. In the case of the ERS scatterometer, the parameters are extracted for each land surface pixel from long backscatter time series by the following: 1) modeling the incidence angle behavior of the backscattering coefficient, 2) correcting seasonal vegetation effects, and 3) extracting the dry and wet backscatter reference values from multiyear time series.

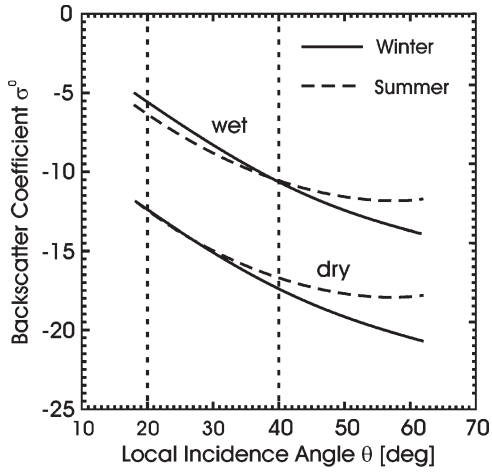

Fig. 2. Dry and wet backscatter reference curves for winter conditions with minimum vegetation cover and summer with maximum vegetation cover. The model parameters were estimated from ERS scatterometer measurements (1991–2007) of a grassland region in Oklahoma (36.86° N; 102.7° W). The two vertical lines indicate the incidence angle range of the ASAR GM (20°–40°).

The description of seasonal vegetation effects makes use of the fact that backscatter may decrease or increase when vegetation grows, depending on whether the attenuation of the soil contribution is more important than the enhanced contribution from the vegetation canopy or vice versa [31]. Since the attenuation of the soil contribution is dominant at low incidence angles while canopy scattering dominates at higher incidence angles, there should be an incidence angle called the "crossover angle" at which both effects balance each other. This is illustrated in Fig. 2, which shows the ERS scatterometer model for a mixed grassland–agricultural area in Oklahoma (36.86° N, 102.7° W). One can see that backscatter increases from winter to summer at higher incidence angles, while at lower incidence angles, backscatter decreases. This is in agreement with vegetation models such as the cloud model introduced by Ulaby and Attema [43]. For dry soil conditions, the crossover angle is set to a value of 25°, which agrees well with the recent observations over a Sahelian test site in Mali made by Baup *et al.* [44]. For wet soils, the crossover angle is 40°.

In the case of the ERS scatterometer, modeling of seasonal effects is facilitated due to the instrument's capability to acquire backscatter measurements at different incidence angles instantaneously. Unfortunately, this is not the case for ASAR GM, which acquires only one backscatter measurement at some incidence angle for a target during each overpass. Therefore, changes in the slope of the $\sigma^0(\theta)$ curve, which are indicative for seasonal vegetation effects, are not directly observable. However, as can be seen in Fig. 2, within the incidence angle range covered by ASAR GM $(20°-40°)$, changes in backscatter due to vegetation growth are, in general, much smaller than changes due to soil moisture. In addition, ASAR GM is commonly operated in HH polarization, which

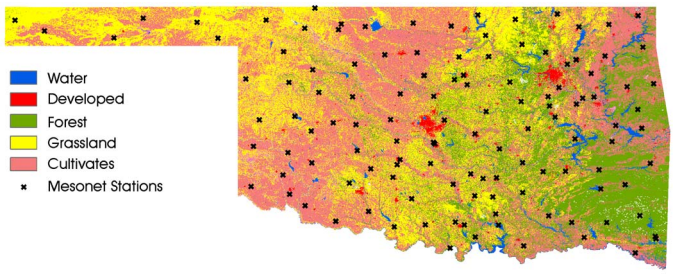

Fig. 3. Oklahoma: Land cover according to the generalized National Land Cover Data classes and MESONET *in situ* soil moisture stations.

penetrates vegetation better than VV polarization as used by the ERS scatterometer [40]. Therefore, the following simplified change detection model is adapted for ASAR GM:

$$\sigma^0(\theta, t) = \sigma^0_{\text{dry}}(30) + \beta(\theta - 30) + Sm_s(t). \tag{2}$$

It is assumed that, in a first approximation, the parameters σ^0_{dry} and S are constant in time because seasonal vegetation effects are expected to be weak for ASAR GM. This assumption may lead to a seasonally varying error of the retrieval. Given the limited incidence angle range of ASAR GM, a linear model is sufficient to describe the incidence angle variation. The slope is characterized by the parameter β, which has the unit decibels per degree. Such a linear model has previously been used by [45]–[48] for modeling the incidence angle dependence of σ^0 observed in ASAR wide swath data.

III. Study Area and Data Sets

A. Study Area

Oklahoma is a federal state of the United States and covers an area of 181 182 km^2. The state is situated mainly in the Great Plains, the broadband of prairie, and steppe covering the inner continental parts of the U.S. [49], [50]. It is characterized by a mostly flat to rolling topography sloping toward the east. The highest point is the Black Mesa with an altitude of 1516 m in the northwestern corner of the panhandle. A generalized land cover map of Oklahoma is shown in Fig. 3.

The climate of Oklahoma is mainly of continental type with a humid subtropical belt in the south. The mean annual temperature is about 15.5 °C, increasing from northwest to southeast. Together with sudden rises and falls of temperature, Oklahoma experiences severe winds, thunderstorms, blizzards, and tornadoes. Precipitation varies strongly from the east to the west. The driest part of the state is the western part of the panhandle with an annual mean precipitation of around 400 mm. From here, the precipitation increases steadily to a value of 1440 mm in the Ouachita Mountains in the southeastern part of Oklahoma. Because of the barrier formed by the Rocky Mountains in the west, precipitation mainly depends on the intrusion of moist air from the Gulf of Mexico. Droughts are a recurring pattern of Oklahoma's climate caused by subnormal rainfall, which can last for several years. Since record keeping began in Oklahoma, five multiyear periods with subnormal rainfall have been reported for the late 1890s, from 1909–18, 1930–40, 1952–58, and 1962–72.

TABLE I
ENVISAT ASAR GM Data Properties

Frequency/Wavelength	5.331 GHz/5.67 cm
Polarization	HH (VV)
Spatial/Temporal Resolution	1000 m/ ≥ 3 days (desc. & asc. orbits)
Radiometric Resolution	1.2 dB
Swath Width	405 km
Incidence Angle Range	20°-40°
Duty Cycle	100%

B. ENVISAT ASAR

This paper uses data acquired by the GM mode of the ASAR onboard of the European Environmental Satellite ENVISAT. ENVISAT was launched on March 1, 2002, and it circles the Earth in a sun-synchronous orbit at an altitude of approximately 800 km with a nominal repeat rate of 35 days. The satellite crosses the equator at 10:00 A.M. in descending node. ASAR can be operated in five main operation modes with selectable polarization. All ASAR modes are exclusive modes, i.e., different modes cannot be acquired at the same time. All ASAR modes except GM are acquired only on user request. GM data are obtained within the so-called background mission, which is active whenever no other data request has been placed by the ground control center. For this paper, 697 GM images in HH polarization covering Oklahoma, USA, acquired within the period December 2004 to December 2006 have been used, which is on average about one image per week. The technical specifications of GM mode are summarized in Table I.

C. In Situ Soil Moisture Data

The Oklahoma MESONET (http://www.mesonet.org/) is a mesoscale environmental monitoring network across Oklahoma [33], [51]. Each station measures air temperature and relative humidity at 1.5 m, wind speed and direction at 10 m, atmospheric pressure, downwelling solar radiation, rainfall, and bare and vegetated soil temperatures at 10 cm below ground level. Over half of the sites include supplemental instruments that measure surface skin temperature [52], net radiation, bare and vegetated soil temperature at 5 cm, and vegetated soil temperature at 30 cm. MESONET data are collected and transmitted to the Oklahoma Climatological Survey every 5 min, where they are quality controlled, distributed, and archived [33], [53].

Soil moisture sensors were installed at four depths (5, 25, 60, and 75 cm) at 60 sites in 1996 and at two depths (5 and 25 cm) at 43 sites in 1999. Some stations were added later. In this paper, we used the 5-cm data from 75 stations for which complete meteorological data records were available. The distribution of these stations is shown in Fig. 3. Data are collected every 30 min, and a series of automated and manual processes performs a quality control and converts the raw data into daily average values of volumetric soil water content [54]. The soil

moisture sensor deployed at Oklahoma MESONET sites is the Campbell Scientific 229-L heat dissipation sensor. This sensor measures its change in temperature after a heat pulse has been introduced [55], [56]. Using the measured temperature difference of the sensor before and after heating (i.e., heat dissipation) and the soil characteristics, hydrological variables such as soil water content and soil matric potential can be calculated. The volumetric water content is determined from a soil water retention curve. Using detailed soil characteristics and soil bulk density measurements collected in the field, soil water retention curves were estimated using a methodology described by Arya and Paris [57]. To guarantee a statewide comparability between measurement stations, a new parameter has been developed based on the measurements of the heat dissipation sensors. This parameter is called fractional water index (FWI) and is a normalized version of the actual measurements of the soil moisture sensors. With the FWI, a statewide analysis of soil moisture conditions and comparisons between individual measurement sites is possible. The FWI is a unitless measure ranging from zero at dry conditions to unity for saturated soils [58].

D. ERS Scatterometer Soil Moisture Data

ERS scatterometer surface soil moisture data have been extracted from the historical archive available at the Vienna University of Technology (http://www.ipf.tuwien.ac.at/radar/). The data have a spatial resolution of 50 km. This soil moisture data set was first published in 2002 [59] and was made freely available to the research community. Various validation studies showed that the quality of the retrieved soil moisture data is good over regions with low to moderate vegetation cover in temperate and tropical climates [12], [16], [60]–[62], while retrieval is of lower quality or not possible in densely forested areas (tropical rain forest), desert and high-latitude areas, and mountainous regions. For example, Pellarin *et al.* [63] compared the ERS-scatterometer-derived surface soil moisture data with the modeled soil moisture data over a half-degree region in Southwestern France. A good root-mean-square error that is equal to 0.06 m^3m^{-3} was found. Furthermore, the data have already been used in various applications, including hydrologic studies [64], [65], precipitation forecasting [66], climate studies [67]–[69], and crop yield forecasting [70].

ERS-1 and ERS-2 scatterometer data have been acquired since the launch of ERS-1 in 1991. However, there is a gap in the ERS-2 time series because of the failures of the ERS-2 gyroscopes in January 2001 and of the tape recorder in June 2003. In North America, data coverage was recovered by switching on the ground receiving stations in Gatineau, Canada, in July 2003 and Miami, USA, in November 2004.

IV. Method

The applicability of the change detection model (2) to estimate soil moisture from ASAR GM time series is tested by estimating the model parameters $\sigma^0_{\mathrm{dry}}(30)$, β, and S; calculating ASAR GM soil moisture data; and comparing these to *in situ* and scatterometer soil moisture data over Oklahoma.

A. Preprocessing

The preprocessing of the ASAR GM data consists of several steps, most importantly geocoding, radiometric correction, and resampling. The geocoding and radiometric correction are done using the software SARscape developed by the Swiss company SARMAP. The software SARscape performs a backward geocoding using the range-Doppler approach described in [71]. Based on precise orbit information (DORIS orbit files) and digital elevation data (Shuttle Radar Topography Mission-improved U.S. Geological Survey GTOPO30 digital elevation model), it reconstructs the sensor position during data acquisition. This procedure does not require ground control points and works without user interaction. Thus, it is possible to process a large number of images fully automatically. As a by-product, the local incidence angle for each image pixel is calculated during the geometric correction process. The radiometric calibration implemented in SARscape involves correction for the scattering area, the antenna gain pattern, and the range spreading loss [72].

In order to facilitate the temporal analysis of ASAR GM data, all images are resampled to a fixed grid and stored in time series files, each covering a 0.5° by 0.5° tile. The grid interval is 15 arc seconds, corresponding to a distance of about 500 m at the equator. The chosen datum is WGS-84, and the origin was set to −180W −90S. The grid and data structure were designed for global processing. The time series files contain, for each acquisition, the date and time of acquisition, the backscattering coefficient in decibels, and the local incidence angle.

B. Incidence Angle Behavior

Radar backscatter generally shows a strong dependence on the local incidence angle. Over bare or sparsely vegetated terrain with smooth soil surfaces, backscatter decreases strongly with increasing incidence angle [73]. With increasing surface roughness and vegetation density, the decrease of σ^0 is less pronounced. Due to the large incidence angle range of the ERS scatterometer $(18°-59°)$, many studies investigated its angular signature for different land cover types. For example, Mougin *et al.* [74] found that the $\sigma^0(\theta)$ function is relatively flat over tropical forests and shrub savanna with slope values of −0.056 and −0.089 dB/deg, respectively, while it is steep over sparse vegetation (−0.13 dB/deg) and bare soil surfaces (−0.21 dB/deg).

The most common approach for investigating the angular behavior of σ^0 has been to fit a linear model to measurements acquired over weekly, monthly, or yearly time intervals. Such an approach has been used for scatterometer [75], [76] and SAR data [45], [77], [78] and is also adapted in this paper. Because the slope β in (2) is constant in time, it is estimated for each grid point by fitting a linear model to all ASAR GM σ^0 measurements from that point. The largest source of uncertainty of this method is related to the concurrent variability of σ^0 due to soil moisture and incidence angle changes. For example, it may happen by pure chance that far-range σ^0 measurement is most often acquired during wet periods, while the near-range σ^0 measurement is acquired during dry conditions. In such a situation, the slope of $\sigma^0(\theta)$ would appear less steep than in

reality, i.e., the absolute value of β would be underestimated. With an increasing number of ASAR GM measurements, such a situation becomes more and more unlikely.

C. Dry and Wet References

The parameters $\sigma^0_{\rm dry}(30)$ and S of the change detection model given by (2) are estimated by analyzing the time series for each grid point. In a first step, all $\sigma^0(\theta)$ measurements are extrapolated to a reference angle of 30° using the slope parameter β

$$\sigma^0(30,t) = \sigma^0(\theta,t) - \beta(\theta - 30). \tag{3}$$

This gives, for each grid point, a time series of $\sigma^0(30)$ values (between 120 and 190 measurements in this study), whereas measurements from frozen and snow covered soil are excluded using the available air temperature data. Using statistical approaches, a low backscatter reference value and a high one are extracted, which, due to the linear relationship between backscatter and soil moisture, are assumed to represent dry ($\sigma^0_{\rm dry}$) and wet ($\sigma^0_{\rm wet}$) soil conditions, respectively. The sensitivity can then be estimated from

$$S = \sigma^0_{\rm wet}(30) - \sigma^0_{\rm dry}(30). \tag{4}$$

The estimation of the two reference values from the $\sigma^0(30)$ sample set is not as straightforward as it may appear. This is because of measurement errors, outliers (e.g., because a GM measurement taken during snow conditions was not correctly identified), and the relatively high noise level of the GM mode. Therefore, the absolute minimum and maximum values of $\sigma^0(30)$ are, in general, poor estimators of $\sigma^0_{\rm dry}$ and $\sigma^0_{\rm wet}$, respectively. One approach would be to select several ASAR acquisitions representing dry and wet conditions, respectively, and averaging over them. The selection could be done on the basis of external soil moisture data such as provided by models or the ERS scatterometer. This approach requires coregistration and resampling of the external soil moisture data to the ASAR images, which is computationally expensive. The simpler approach adapted here is to assume that the numbers of GM measurements taken during dry ($N_{\rm dry}$) and wet ($N_{\rm wet}$) soil conditions are approximately known. By sorting the $\sigma^0_i(30)$ in ascending order and by calculating the average over the $N_{\rm dry}$-lowest $\sigma^0_i(30)$ values, the dry backscatter reference can be estimated using

$$\sigma^0_{\rm dry}(30) \approx \frac{1}{N_{\rm dry}} \sum_{i=1}^{N_{\rm dry}} \sigma^0_i(30). \tag{5}$$

Correspondingly, by averaging the $N_{\rm wet}$-highest $\sigma^0_i(30)$ values, the wet reference value is obtained

$$\sigma^0_{\rm wet}(30) \approx \frac{1}{N_{\rm wet}} \sum_{i=N-N_{\rm wet}}^{N} \sigma^0_i(30) \tag{6}$$

where N is the total number of measurements. The numbers of GM measurements $N_{\rm dry}$ and $N_{\rm wet}$ are estimated for each grid point from the historical ERS scatterometer soil moisture archive using

$$N_{\rm dry} \approx N_{\rm GM} \frac{N(m_s < 5\%)}{N_{\rm SCAT}} \tag{7}$$

$$N_{\rm wet} \approx N_{\rm GM} \frac{N(m_s > 95\%)}{N_{\rm SCAT}} \tag{8}$$

where $N_{\rm GM}$ is the total number of GM measurements at the specific grid point, $N_{\rm SCAT}$ is the number of ERS scatterometer retrieved soil moisture values m_s over the same grid point, $N(m_s < 5\%)$ is the number of ERS soil moisture data below 5%, and $N(m_s > 95\%)$ is the number of ERS soil moisture data above 95%. The resolution difference between ASAR and the ERS scatterometer is not regarded to be a problem because the probabilities for observing dry and wet conditions are driven by climatic conditions acting across a wide range of spatial scales [79].

D. Soil Moisture Retrieval

Using the estimated model parameters $\sigma^0_{\rm dry}$ and S, a relative surface soil moisture index is retrieved from the extrapolated ASAR GM measurements

$$m_s(t) = \frac{\sigma^0(30,t) - \sigma^0_{\rm dry}(30)}{S}. \tag{9}$$

For characterizing the temporal agreement, the ASAR-GM-retrieved soil moisture index time series are compared to the *in situ* and ERS scatterometer soil moisture data over the MESONET stations. The following statistical measures are calculated for each time series pairs for each of the 75 MESONET station: correlation coefficient (R), the bias, and the standard deviation (SD). The bias between two soil moisture data sets x and y is given by

$$\text{bias} = \frac{1}{M} \sum_{j=1}^{M} (y(t_j) - x(t_j)) \tag{10}$$

where M is the number of concurrent measurements at times t_j. The SD is calculated as follows:

$$\text{SD} = \sqrt{\frac{1}{M-1} \sum_{j=1}^{M} (y(t_j) - x(t_j) - \text{bias})^2}. \tag{11}$$

E. Error Estimation

The retrieval error of m_s is determined by the noise of the ASAR GM backscatter measurements and uncertainties of the model parameters. Denoting the noise of the GM backscatter measurements by $\Delta\sigma^0$ and the errors of the model parameters β, $\sigma^0_{\rm dry}(30)$, and $\sigma^0_{\rm wet}(30)$ by $\Delta\beta$, $\Delta\sigma^0_{\rm dry}$, and $\Delta\sigma^0_{\rm wet}$, respectively, the retrieval error Δm_s can be estimated with

$$\Delta m_s^2 \approx \left(\frac{\Delta\sigma^0}{S}\right)^2 + \left(\frac{(\theta-30)\Delta\beta}{S}\right)^2 + \ldots + \left(\frac{(m_s-1)\,\Delta\sigma^0_{\rm dry}}{S}\right)^2 + \left(\frac{m_s \Delta\sigma^0_{\rm wet}}{S}\right)^2 \tag{12}$$

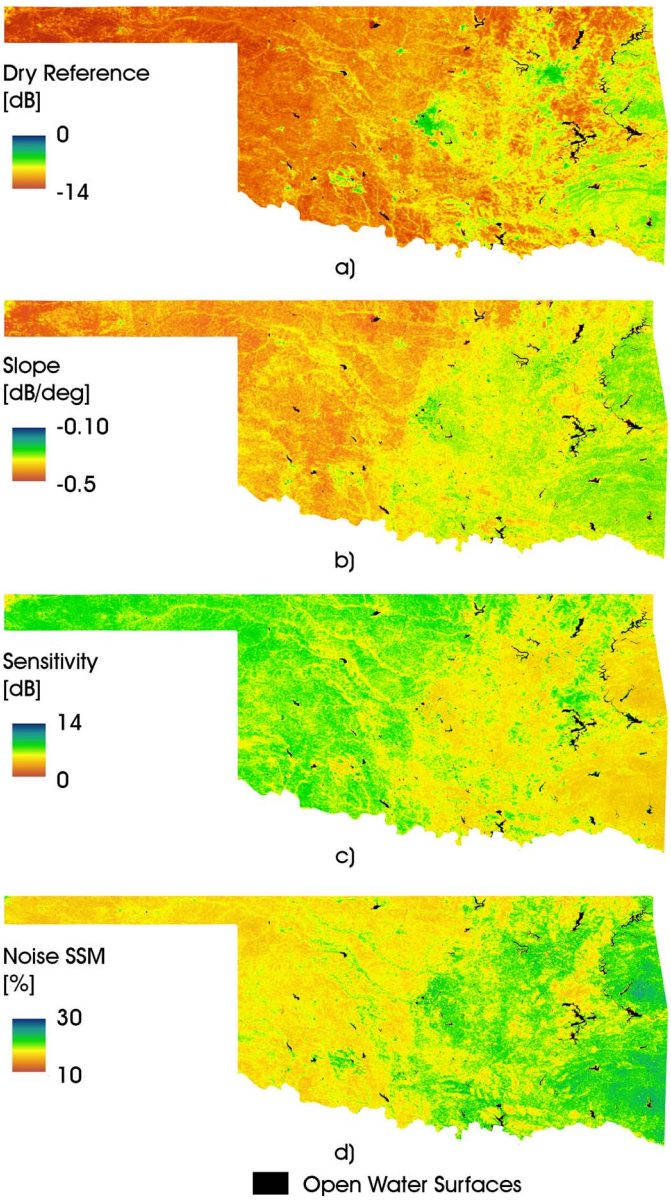

Fig. 4. (a)–(c) Backscatter model parameters extracted from ASAR GM time series and (d) estimated maximum retrieval error over Oklahoma [(black) masked out water surfaces]. (a) Dry backscatter reference σ^0_{dry} in decibels. (b) Slope β in dB/deg. (c) Sensitivity S in decibels. (d) Maximum surface soil moisture retrieval error Δm_s in percent.

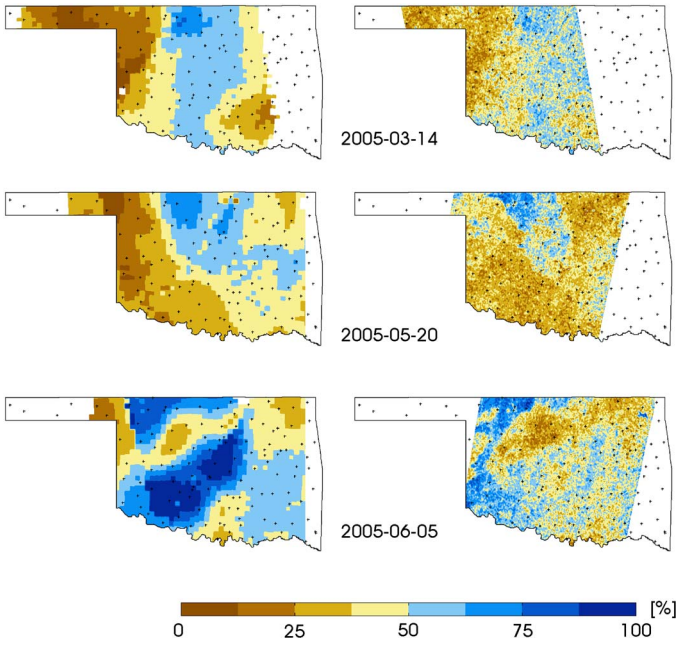

Fig. 5. Surface soil moisture maps of Oklahoma retrieved from (left) ERS scatterometer and (right) ASAR GM measurements for three different dates in spring 2005.

whereas it is assumed that the errors are independent of each other. While the noise of the GM backscatter measurements is known ($\Delta\sigma^0 = 1.2$ dB), the uncertainties of the model parameters are unknown and need to be estimated based on an understanding of the potential error sources. First, errors may occur due to the limited number and irregular temporal distribution of available ASAR measurements over the four seasons. Second, erroneous backscatter values may be present in the time series (e.g., ASAR processing errors). Third, the statistical methods used for calculating β, $\sigma^0_{\mathrm{dry}}(30)$, and $\sigma^0_{\mathrm{wet}}(30)$ are, of course, also uncertain to some extent. Finally, the neglect of seasonal vegetation cover effects is expected to cause seasonally varying errors in all three model parameters. Considering, in particular, the error due to vegetation phenology, we assume a high relative error of β on the order of 10%, i.e., $\Delta\beta = 0.1\,\beta$. Moreover, the errors $\Delta\sigma^0_{\mathrm{dry}}$ and $\Delta\sigma^0_{\mathrm{wet}}$ are assumed to be 10% relative to the observed dynamic range of the backscatter measurements, i.e., $\Delta\sigma^0_{\mathrm{dry}} = \Delta\sigma^0_{\mathrm{wet}} = 0.1$ S.

By substituting these assumptions into (12) and selecting values for θ and m_s, the retrieval error Δm_s can thus be estimated for every pixel. The maximum error occurs when measurements are taking in either near ($\theta = 20^\circ$) or far ($\theta = 40^\circ$) range and at dry ($m_s = 0$) or wet ($m_s = 1$) soil moisture conditions, respectively. Thus, the maximum retrieval error is estimated to be

$$\Delta m_{s,\max} \approx \sqrt{\left(\frac{1.2}{S}\right)^2 + \left(\frac{\beta}{S}\right)^2 + 0.01}. \qquad (13)$$

V. Results and Discussion

A. Spatial Patterns

The spatial images of the backscatter model parameters $\sigma^0_{\mathrm{dry}}(30)$, β, and S extracted from the ASAR GM time series are shown in Fig. 4(a)–(c). Fig. 4(d) shows the estimated maximum error of m_s calculated using (13). The observed east to west gradient in these images corresponds well to the climatic and physiographic gradient in Oklahoma. Some artifacts can be observed at the borders of GM swaths, particularly in the β image [Fig. 4(b)]. However, these artifacts are comparably small (much smaller than the assumed errors) and are expected to vanish when more GM data become available.

When comparing Fig. 4 to the land cover map shown in Fig. 3, it can be seen that vegetation has a strong impact on all parameters. As expected, $\sigma^0_{\mathrm{dry}}(30)$ increases with increasing vegetation biomass, while S and the absolute value of β

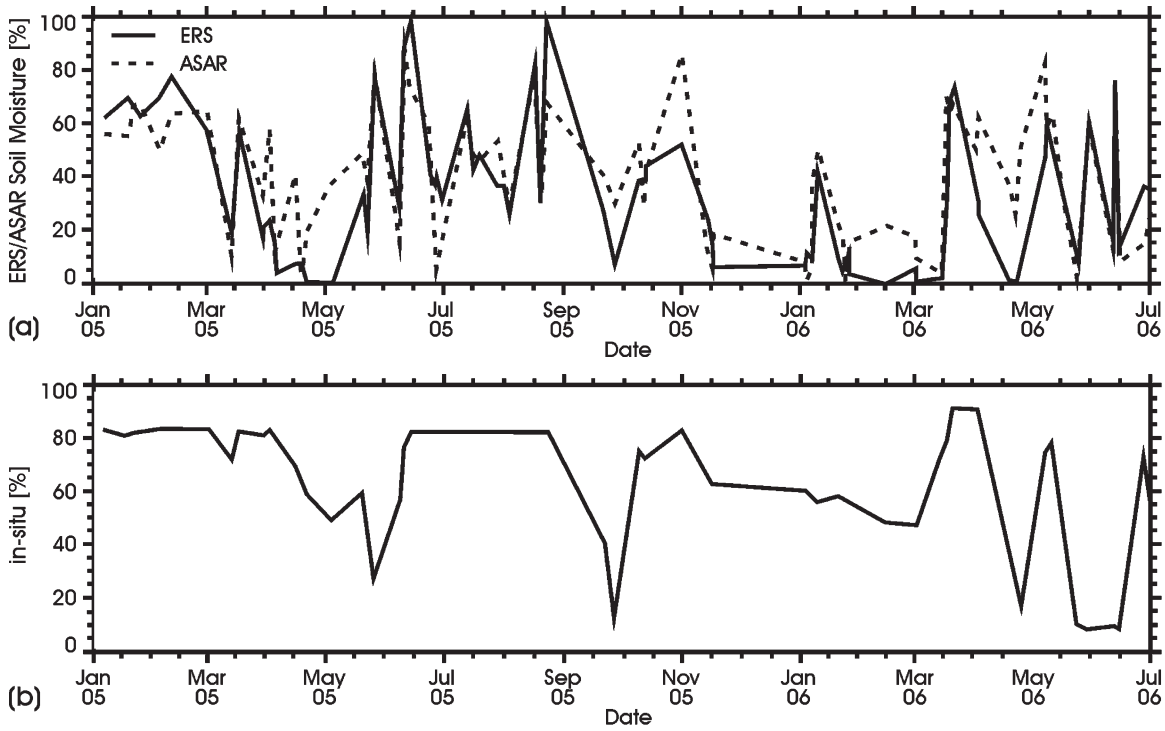

Fig. 6. (a) Soil moisture time series from (dashed line) ASAR GM and (solid line) ERS scatterometer and (b) *in situ* measurements at the MESONET station LAHO for the period January 2005 to July 2006. The gray areas show time periods with $T_{\min} < 1$ °C, when frozen soil and/or snow may have occurred. Under such conditions, the satellite-derived soil moisture data must be discarded.

decrease. Because of the strong influence of vegetation, all three parameters are correlated. The spatial correlation (R) is 0.80 between $\sigma^0_{\rm dry}(30)$ and β, -0.86 between $\sigma^0_{\rm dry}(30)$ and S, and -0.82 between β and S. Aside from vegetation, also built-up areas have a strong influence on the backscatter parameters in Fig. 4. As was observed with the ERS scatterometer [31], urban areas have a similar influence on the backscatter parameters as vegetation, i.e., the presence of built-up areas tends to increase $\sigma^0_{\rm dry}(30)$ and decrease S and the absolute value of β.

The spatial pattern of the estimated maximum retrieval error, as shown in Fig. 4(d), reflects the patterns of S and β. Overall, the estimated error is quite high with maximum values above 20% in the more densely vegetated areas in the eastern part of Oklahoma and values of around 15% in the grassland- and agriculture-dominated areas. The mean is 18%. Because S is generally smaller than 12 dB and β takes on values between -0.4 and -0.1 dB/deg, one can see from (13) that, even when assuming very high model parameter errors to account for the neglect of seasonal vegetation cover effects, the retrieval error is dominated by the noise of the ASAR GM measurements. This suggests that several pixels should be averaged to decrease the noise level, which is done at the expense of the spatial resolution of the soil moisture maps.

Exemplary maps showing the spatial distribution of soil moisture extracted from the ERS scatterometer data and the ASAR GM data over Oklahoma are shown in Fig. 5. The overall patterns of low and high soil moisture are similar in the soil moisture maps from both sensors. The most apparent difference is the spatial resolution between the ERS soil moisture and the ASAR GM soil moisture. Due to this difference, the ERS soil moisture maps appear much smoother than the ASAR GM soil moisture maps. This effect is enhanced by the high ASAR GM noise level.

B. Temporal Dynamics

When comparing the soil moisture time series from the *in situ* stations with that of the ASAR GM and ERS scatterometer, one has to bear in mind the large-scale differences. While the *in situ* measurements only represent an area of about 0.1 to 10 dm^2, the satellite data represent areas of 1 km^2 (ASAR GM) and 2500 km^2 (ERS scatterometer). The comparison is nevertheless possible because soil moisture patterns tend to persist in time, which is a phenomenon usually referred to as temporal stability [79]. Therefore, soil moisture measured at local scale is often correlated with the mean soil moisture content over larger areas. Nevertheless, the temporal correlation can be lost when small-scale hydrologic processes counteract the influence of the large-scale atmospheric forcing. Therefore, a low correlation observed between soil moisture time series representing different spatial scales does not necessarily point to a poor quality of the measurements but might be due to the scaling problem.

A visual comparison of the temporal evolution of the ASAR GM soil moisture index with the ERS scatterometer time series is shown in Fig. 6(a), exemplified for the MESONET station "LAHO." To ensure comparability, only ERS scatterometer data and ASAR GM data pairs obtained within 2 h from each other were taken into account during the validation. The lower part of the figure [Fig. 6(b)] shows the concurrent FWI values representing the *in situ* soil moisture. It can be seen that the temporal evolution of the two remotely sensed soil moisture

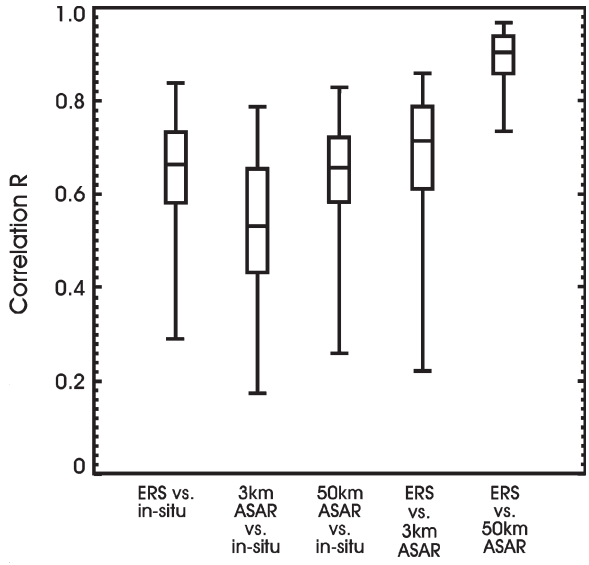

Fig. 7. Correlation (R) between four soil moisture data sets for 75 Oklahoma MESONET stations: ERS scatterometer versus *in situ*, 3-km ASAR GM versus *in situ*, 50-km ASAR GM versus *in situ*, ERS scatterometer versus 3-km ASAR GM, and ERS scatterometer versus 50-km ASAR GM.

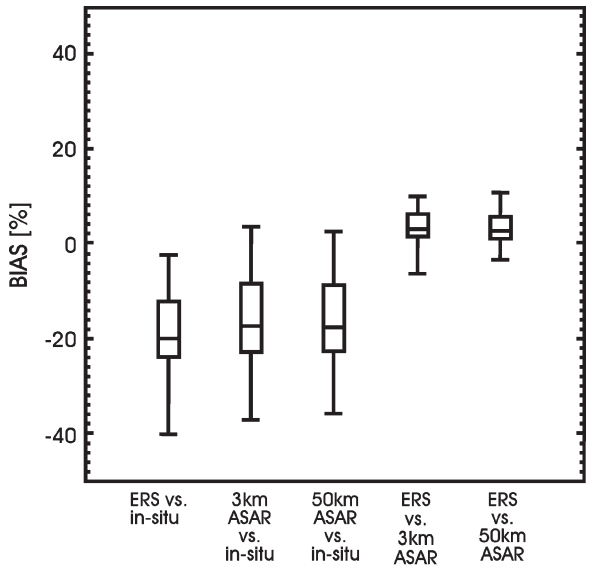

Fig. 8. Bias between four soil moisture data sets for 75 Oklahoma MESONET stations. See also Fig. 7.

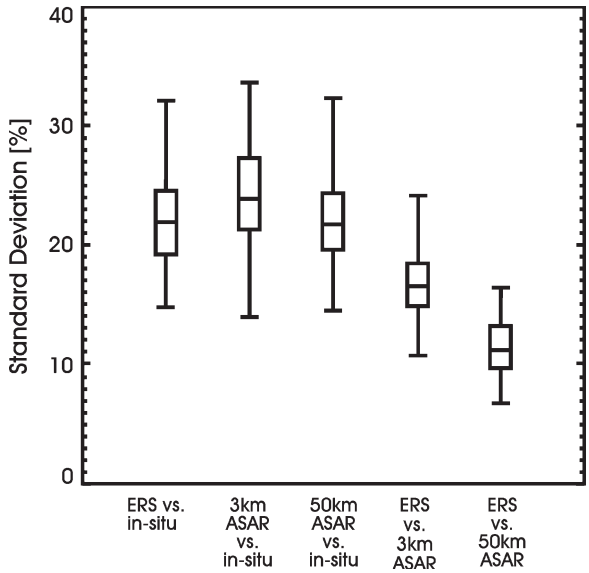

Fig. 9. SD between four soil moisture data sets for 75 Oklahoma MESONET stations. See also Figs. 7 and 8.

data sets agrees reasonably well with the *in situ* measurements, even though the transitions from dry to wet are, in general, more pronounced in the FWI data. A similar behavior can be observed for other stations.

For a more quantitative assessment of the ASAR GM soil moisture index with respect to the *in situ* and ERS scatterometer soil moisture measurements, statistical parameters were calculated for the three data pair combinations for each of the 75 MESONET stations. All acquisitions, for which snow or frozen soil conditions may have occurred (minimum daily temperature $< 1\ ^{\circ}$C), were removed before the calculation of the statistics using meteorological data. To account for the high ASAR GM noise level, ASAR GM soil moisture time series were extracted from a 3×3 pixel window centered on the location of the MESONET measurement stations. The resulting spatial resolution is about 3 km. The ASAR data were also averaged to 50 km to enable a comparison of ASAR and the ERS scatterometer at the same spatial scale.

The results for the correlation coefficient R between *in situ*, 3-km ASAR, 50-km ASAR, and ERS scatterometer are summarized in Fig. 7 with the help of box plots that show, for each data pair combination, the smallest R value, the lower quartile ($Q1$), the median ($Q2$), the upper quartile ($Q3$), and the largest R value for the 75 MESONET stations. The absolute values and spread of R are comparable to the results observed in previous studies, where medium to coarse-resolution satellite data were compared to pointlike *in situ* measurements and against each other [8]. More interesting than the absolute values is how ASAR compares relative to the ERS scatterometer data. As one can see in Fig. 7, even though the scale gap from the 3-km ASAR to the *in situ* measurements is less pronounced than in the case of the ERS scatterometer, the correlation for the 3-km ASAR index against the *in situ* measurements is, in general, somewhat weaker than for the ERS scatterometer. The error analysis suggests that this is mainly due to the much higher noise level of ASAR GM compared to the ERS scatterometer and, to a lesser extent, due to the neglect of seasonal vegetation cover effects in the ASAR GM backscatter model. This is confirmed by the fact that the results for the 50-km ASAR and the ERS scatterometer data are very close. Nevertheless, even at the 3-km scale, the differences are within reasonable limits, and the good correlation to the ERS scatterometer data shows that ASAR carries relevant information about soil moisture changes at a spatial resolution finer than the ERS scatterometer.

The results for the bias are shown in Fig. 8. It can be observed that, while there is no significant bias between ASAR GM and ERS scatterometer, the bias toward the *in situ* measurements is substantial for both satellite data sets. This result is not unexpected, given that many previous studies found substantial

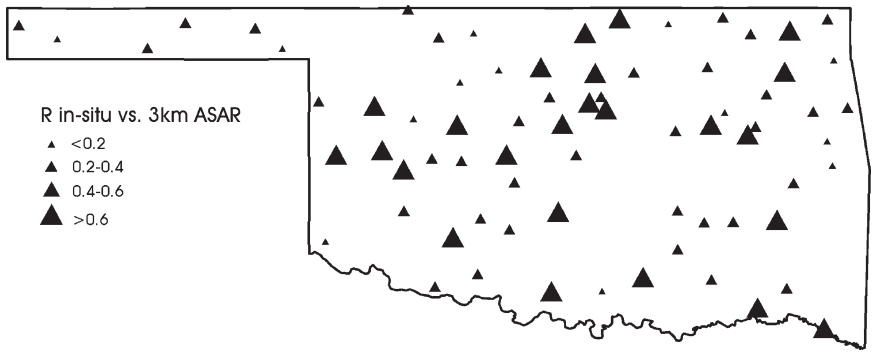

Fig. 10. Spatial distribution of correlation R between *in situ* and 3-km ASAR soil moisture.

differences between the absolute levels of different soil moisture data sets, may they be derived from remote sensing, *in situ* networks, or models [80]. Therefore, techniques like the cumulative distribution function are, in general, used in data assimilation for matching observed and modeled soil moisture data [81].

Finally, the results for the SD as defined by (11) are shown in Fig. 9. The results mirror the results obtained for the correlation, i.e., SD is smallest for the comparison of 50-km ASAR versus ERS scatterometer and highest for 3-km ASAR versus *in situ*. The values for ASAR GM are somewhat higher than the estimated maximum noise of the retrieval error. This is related to the scaling problem (from point scale to 3 and 50 km, respectively) and the fact that each data set has its own errors. Consider two soil moisture data sets that have comparable absolute errors. Then, their real error can be estimated by dividing the observed SD between the two data sets with $\sqrt{2}$. Therefore, it is estimated that the real relative error of ASAR GM lies, in general, in the range from 10% to 20%. For a soil with a porosity of 0.4, this translates into an error of the volumetric soil moisture content on the order of 0.04 to 0.08 m^3m^3. This compares well with the findings from the validation studies with the ERS scatterometer surface soil moisture data [8], [63], [80].

Finally, the dependence of the results on land cover has been investigated. Fig. 10 shows a map of the correlation between the 3-km ASAR GM data and the *in situ* data over the 75 MESONET stations. One can see that, due to the scaling problem, the R values may change strongly between neighboring stations. This variability may, to some extent, hide changes in R due to different land cover. Nevertheless, it is remarkable that, from the grassland-dominated east to the forested west, no clear trends in R can be observed. Moreover, cultivated areas do not have a clear impact even though their phenology is different from natural vegetation. This suggests that the algorithm successfully accounts for different land cover types.

VI. Conclusion

Many studies have demonstrated that change detection methods can successfully be applied to scatterometer and SAR backscatter time series to monitor soil moisture changes [26]. Yet, in the case of SAR, most studies have been confined to basin-scale test areas because SAR satellite systems have, in general, not been designed to obtain repetitive and continuous worldwide coverage. ENVISAT is the first satellite with a ScanSAR mode that can be operated continuously. Potentially, this so-called GM mode can achieve a daily global coverage of about 35%, but in reality, it is much less because GM mode cannot be operated in parallel to any of the other ASAR modes. Nevertheless, most land surface areas have already been covered more than 100 times. Therefore, ENVISAT ASAR GM offers, for the first time, the possibility to retrieve soil moisture at a global scale with a spatial resolution on the order of 1 km.

To test the hypothesis that ASAR GM is a useful tool for monitoring soil moisture over large regions, a change detection method developed for the ERS scatterometer [30]–[32] was adapted for use with ASAR GM. The method uses a model that describes backscatter from vegetated land surfaces in terms of three empirical backscatter parameters and the relative surface soil moisture content. The three parameters can be estimated by analyzing ASAR GM time series for each grid point. The application of the method to 697 ASAR GM images acquired over Oklahoma (181 182 km^2) demonstrated that the three parameters reflect spatial patterns of vegetation and land cover well. An error analysis showed that the retrieval error is dominated by the high noise level of the ASAR GM backscatter measurements (1.2 dB), while a smaller seasonally varying error component is expected to be present due to the neglect of seasonal vegetation cover effects in the backscatter model.

The comparison of the ASAR GM soil moisture time series with ERS scatterometer and *in situ* soil moisture data over the Oklahoma MESONET suggests that, due to the high noise, the quality of ASAR GM soil moisture index is not as good as that of the ERS scatterometer. Therefore, some spatial averaging to 3–10 km is recommended to reduce the noise of the ASAR GM soil moisture images. Moreover, the retrievals may have a spatially variable bias due to uncertainties related to the estimation of the dry and wet backscatter references. Nevertheless, ASAR GM allows resolving spatial details in the soil moisture patterns not observable in the ERS scatterometer measurements while still retaining the basic capability of the ERS scatterometer to capture temporal trends.

Because of the worldwide availability of ASAR GM time series, ASAR GM can be used for testing the capability of multitemporal change detection approaches for spaceborne ScanSAR systems on a global scale. The first results obtained over the southern African continent [82], [83] indicate that

the method presented in this paper is transferable to continental scales and different climatic zones. Further research is required to understand retrieval biases and temporal errors caused by neglecting seasonal vegetation effects. Moreover, the degree of spatial averaging required by different applications such as hydrology and meteorology needs to be investigated. ASAR GM soil moisture data from Oklahoma, southern Africa, and Australia can be obtained from the website of TU Wien http://www.ipf.tuwien.ac.at/radar/share/.

ACKNOWLEDGMENT

The authors would like to thank the reviewers for their insightful comments and the European Space Agency for providing the ENVISAT ASAR GM data. This study has been carried out within the framework of the SHARE project.

REFERENCES

[1] N. W. Arnell, "Climate change and global water resources," *Glob. Environ. Change*, vol. 9, no. 1, pp. S31–S49, Oct. 1999.

[2] M. Sivapalan, K. Takeuchi, S. W. Franks, V. K. Gupta, H. Karambiri, V. Lakshmi, X. Liang, J. J. McDonnell, E. M. Mendiondo, P. E. O'Connell, T. Oki, J. W. Pomeroy, D. Schertzer, S. Uhlenbrook, and E. Zehe, "IAHS decade on Predictions in Ungauged Basins (PUB), 2003–2012: Shaping an exciting future for the hydrologic sciences," *Hydrol. Sci. J.*, vol. 48, no. 6, pp. 857–880, 2003.

[3] C. J. Vörösmarty, "Global water assessment and potential contributions from Earth Systems Science," *Aquat. Sci.*, vol. 64, no. 4, pp. 328–351, 2002.

[4] J. P. Walker, G. R. Willgoose, and J. D. Kalma, "*In situ* measurement of soil moisture: A comparison of techniques," *J. Hydrol.*, vol. 293, no. 1–4, pp. 85–99, Jun. 2004.

[5] A. Robock, K. Y. Vinnikov, G. Srinivasan, J. K. Entin, S. E. Hollinger, N. A. Speranskaya, S. Liu, and A. Namkhai, "The global soil moisture data bank," *Bull. Amer. Meteorol. Soc.*, vol. 81, no. 6, pp. 1281–1299, Jun. 2000.

[6] E. T. Engman and N. S. Chauhan, "Status of microwave soil moisture measurements with remote sensing," *Remote Sens. Environ.*, vol. 51, no. 1, pp. 189–198, Jan. 1995.

[7] J. R. Eagleman and F. T. Ulaby, "Remote sensing of soil moisture by Skylab radiometer and scatterometer sensors," *J. Astronaut. Sci.*, vol. 23, pp. 147–159, Apr. 1975.

[8] W. Wagner, V. Naeimi, K. Scipal, R. de Jeu, and J. Martinez-Fernandez, "Soil moisture from operational meteorological satellites," *Hydrogeol. J.*, vol. 15, no. 1, pp. 121–131, Feb. 2007.

[9] Y. Liu, R. A. M. de Jeu, A. I. J. M. van Dijk, and M. Owe, "TRMM-TMI satellite observed soil moisture and vegetation density (1998–2005) show strong connection with El Nino in eastern Australia," *Geophys. Res. Lett.*, vol. 34, p. L15 401, 2007.

[10] R. H. Reichle, R. D. Koster, P. Liu, S. P. P. Mahanama, E. G. Njoku, and M. Owe, "Comparison and assimilation of global soil moisture retrievals from the advanced microwave scanning radiometer for the Earth Observing System (AMSR-E) and the scanning multichannel microwave radiometer (SMMR)," *J. Geophys. Res.*, vol. 112, p. D09 108, 2007.

[11] E. G. Njoku, T. J. Jackson, V. Lakshmi, T. K. Chan, and S. V. Nghiem, "Soil moisture retrieval from AMSR-E," *IEEE Trans. Geosci. Remote Sens.*, vol. 41, no. 2, pp. 215–229, Feb. 2003.

[12] W. Wagner, K. Scipal, C. Pathe, D. Gerten, W. Lucht, and B. Rudolf, "Evaluation of the agreement between the first global remotely sensed soil moisture data with model and precipitation data," *J. Geophys. Res.*, vol. 108, no. D19, p. 4611, Oct. 2003.

[13] M. Zribi, C. Andre, and B. Dechambre, "A method for soil moisture estimation in western Africa based on the ERS scatterometer," *IEEE Trans. Geosci. Remote Sens.*, vol. 46, no. 2, pp. 438–448, Feb. 2008.

[14] J. Wen and Z. B. Su, "A time series based method for estimating relative soil moisture with ERS wind scatterometer data," *Geophys. Res. Lett.*, vol. 30, no. 7, p. 1397, Apr. 2003.

[15] C. Rüdiger, J.-C. Calvet, C. Gruhier, T. Holmes, R. de Jeu, and W. Wagner, "An intercomparison of ERS-Scat and AMSR-E soil moisture observations with model simulations over France," *J. Hydrometeorol.* DOI: 10.1175/2008JHM997.1.

[16] W. Crow and X. Zhan, "Continental-scale evaluation of remotely sensed soil moisture products," *IEEE Geosci. Remote Sens. Lett.*, vol. 4, no. 3, pp. 451–455, Jul. 2007.

[17] Y. H. Kerr, P. Waldteufel, J.-P. Wigneron, J. Martinuzzi, J. Font, and M. Berger, "Soil moisture retrieval from space: The Soil Moisture and Ocean Salinity (SMOS) mission," *IEEE Trans. Geosci. Remote Sens.*, vol. 39, no. 8, pp. 1729–1735, Aug. 2001.

[18] I. H. Woodhouse, *Introduction to Microwave Remote Sensing*. Boca Raton, FL: CRC Press, 2006.

[19] D. Entekhabi, E. G. Njoku, P. Houser, M. Spencer, T. Doiron, K. Yunjin, J. Smith, R. Girard, S. Belair, W. Crow, T. J. Jackson, Y. H. Kerr, J. S. Kimball, R. Koster, K. C. McDonald, P. E. O'Neill, T. Pultz, S. W. Running, S. Jiancheng, E. Wood, and J. van Zyl, "The Hydrosphere State (Hydros) satellite mission: An Earth system pathfinder for global mapping of soil moisture and land freeze/thaw," *IEEE Trans. Geosci. Remote Sens.*, vol. 42, no. 10, pp. 2184–2195, Oct. 2004.

[20] Y. H. Kerr, "Soil moisture from space: Where are we?" *Hydrogeol. J.,* vol. 15, no. 1, pp. 117–120, Feb. 2007.

[21] C. Oliver and S. Quegan, *Understanding Synthetic Aperture Radar Images*. Boston, U.K.: Artech House, 1998.

[22] G. Satalino, F. Mattia, M. W. J. Davidson, T. Le Toan, G. Pasquariello, and M. Borgeaud, "On current limits of soil moisture retrieval from ERS-SAR data," *IEEE Trans. Geosci. Remote Sens.*, vol. 40, no. 11, pp. 2438–2447, Nov. 2002.

[23] F. T. Ulaby, R. K. Moore, and A. K. Fung, *Microwave Remote Sensing: Active and Passive, Vol. III: From Theory to Applications*. Norwood, MA: Artech House, 1986.

[24] N. Baghdadi, M. Aubert, O. Cerdan, L. Franchisteguy, C. Viel, E. Martin, M. Zribi, and J. F. Desprats, "Operational mapping of soil moisture using synthetic aperture radar data: Application to the Touch basin (France)," *Sensors*, vol. 7, pp. 2458–2483, Oct. 2007.

[25] M. S. Moran, D. C. Hymer, J. Qi, and E. E. Sano, "Soil moisture evaluation using multi-temporal synthetic aperture radar (SAR) in semi-arid rangeland," *Agric. For. Meteorol.*, vol. 105, no. 1, pp. 69–80, Nov. 2000.

[26] W. Wagner, G. Blöschl, P. Pampaloni, J.-C. Calvet, B. Bizzarri, J.-P. Wigneron, and Y. Kerr, "Operational readiness of microwave remote sensing of soil moisture for hydrologic applications," *Nord. Hydrol.*, vol. 38, no. 1, pp. 1–20, 2007.

[27] M. Suess, S. Riegger, W. Pitz, and R. Werninghaus, "TerraSAR-X—Design and performance," in *Proc. 4th EUSAR*, Cologne, Germany, 2002, pp. 49–52.

[28] R. Bamler and M. Eineder, "ScanSAR processing using standard high precision SAR algorithms," *IEEE Trans. Geosci. Remote Sens.*, vol. 34, no. 1, pp. 212–218, Jan. 1996.

[29] P. Lecomte, "The ERS scatterometer instrument and the on-ground processing of its data," in *Proc. Emerg. Scatterometer Appl.: From Res. Operations*, Noordwijk, The Netherlands, 1998, pp. 241–260.

[30] W. Wagner, J. Noll, M. Borgeaud, and H. Rott, "Monitoring soil moisture over the Canadian Prairies with the ERS scatterometer," *IEEE Trans. Geosci. Remote Sens.*, vol. 37, no. 1, pp. 206–216, Jan. 1999.

[31] W. Wagner, G. Lemoine, M. Borgeaud, and H. Rott, "A study of vegetation cover effects on ERS scatterometer data," *IEEE Trans. Geosci. Remote Sens.*, vol. 37, no. 2, pp. 938–948, Mar. 1999.

[32] W. Wagner, G. Lemoine, and H. Rott, "A method for estimating soil moisture from ERS scatterometer and soil data—Empirical data and model results," *Remote Sens. Environ.*, vol. 70, no. 2, pp. 191–207, Nov. 1999.

[33] R. A. McPherson, C. Fiebrich, K. C. Crawford, R. L. Elliott, J. R. Kilby, D. L. Grimsley, J. E. Martinez, J. B. Basara, B. G. Illston, D. A. Morris, K. A. Kloesel, S. J. Stadler, A. D. Melvin, A. J. Sutherland, and H. Shrivastava, "Statewide monitoring of the mesoscale environment: A technical update on the Oklahoma Mesonet," *J. Atmos. Ocean. Technol.*, vol. 24, no. 3, pp. 301–321, Mar. 2007.

[34] R. K. Raney, "Radar fundamentals: Technical perspective," in *Principles and Applications of Imaging Radar*, F. M. Henderson and A. J. Lewis, Eds. New York: Wiley, 1998.

[35] A. Smith, K. Scipal, W. Wagner, and A. Cracknell, "Active microwave systems for monitoring drought stress," in *Monitoring and Predicting Agricultural Drought: A Global Study*, V. Boken, A. Cracknell, and R. Heathcote, Eds. New York: Oxford Univ. Press, 2005.

[36] M. W. J. Davidson, T. Le Toan, F. Mattia, G. Satalino, T. Manninen, and M. Borgeaud, "On the characterization of agricultural soil roughness for radar remote sensing studies," *IEEE Trans. Geosci. Remote Sens.*, vol. 38, no. 2, pp. 630–640, Mar. 2000.

[37] J. Walker, P. Houser, and G. Willgoose, "Active microwave remote sensing for soil moisture measurement: A field evaluation using ERS-2," *Hydrol. Process.*, vol. 18, no. 11, pp. 1975–1997, Aug. 2004.
[38] N. Baghdadi and M. Zribi, "Evaluation of radar backscatter models IEM, OH and Dubois using experimental observations," *Int. J. Remote Sens.*, vol. 27, no. 18, pp. 3831–3852, Sep. 2006.
[39] G. Macelloni, G. Nesti, P. Pampaloni, S. Sigismondi, D. Tarchi, and S. Lolli, "Experimental validation of surface scattering and emission models," *IEEE Trans. Geosci. Remote Sens.*, vol. 38, no. 1, pp. 459–469, Jan. 2000.
[40] S. C. M. Brown, S. Quegan, K. Morrison, J. C. Bennett, and G. Cookmartin, "High-resolution measurements of scattering in wheat canopies—Implications for crop parameter retrieval," *IEEE Trans. Geosci. Remote Sens.*, vol. 41, no. 7, pp. 1602–1610, Jul. 2003.
[41] J.-M. Martinez, N. Floury, T. Le Toan, A. Beaudoin, M. T. Hallikainen, and M. Mäkynen, "Measurements and modeling of vertical backscatter distribution in forest canopy," *IEEE Trans. Geosci. Remote Sens.*, vol. 38, no. 2, pp. 710–719, Mar. 2000.
[42] D. Hillel, *Introduction to Soil Physics*. San Diego, CA: Academic, 1982.
[43] F. T. Ulaby and E. Attema, "Vegetation modeled as a water cloud," *Radio Sci.*, vol. 13, no. 2, pp. 357–364, 1978.
[44] F. Baup, E. Mougin, P. de Rosnay, F. Timouk, and I. Chênere, "Surface soil moisture estimation over the AMMA Sahelian site in Mali using ENVISAT/ASAR data," *Remote Sens. Environ.*, vol. 109, no. 4, pp. 473–481, Aug. 2007.
[45] A. Loew, R. Ludwig, and W. Mauser, "Derivation of surface soil moisture from ENVISAT ASAR wide swath and image mode data in agricultural areas," *IEEE Trans. Geosci. Remote Sens.*, vol. 44, no. 4, pp. 889–899, Apr. 2006.
[46] I. Champion, "Simple modelling of radar backscattering coefficient over a bare soil: Variation with incidence angle, frequency and polarization," *Int. J. Remote Sens.*, vol. 17, no. 4, pp. 783–800, 1996.
[47] M. S. Moran, C. D. Peters-Lidar, J. M. Watts, and S. McElroy, "Estimating soil moisture at the watershed scale with satellite-based radar and land surface models," *Can. J. Remote Sens.*, vol. 30, no. 5, pp. 805–826, Oct. 2004.
[48] M. R. Sahebi, F. Bonn, and G. H. J. Gwyn, "Estimation of the moisture content of bare soil from RADARSAT-1 SAR using simple empirical models," *Int. J. Remote Sens.*, vol. 24, no. 12, pp. 2575–2582, Jan. 2003.
[49] J. H. Paterson, *North America. A Geography of the United States and Canada*. New York: Oxford Univ. Press, 1994.
[50] T. L. McKnight, *Regional Geography of the United States and Canada*. Englewood Cliffs, NJ: Prentice-Hall, 1992.
[51] F. V. Brock, K. C. Crawford, R. L. Elliott, G. W. Cuperus, S. Stadler, H. L. Johnson, and M. D. Eilts, "The Oklahoma Mesonet: A technical overview," *J. Atmos. Ocean. Technol.*, vol. 12, no. 1, pp. 5–19, Feb. 1995.
[52] C. A. Fiebrich, J. E. Martinez, J. A. Brotzge, and J. B. Basara, "The Oklahoma Mesonet's skin temperature network," *J. Atmos. Ocean. Technol.*, vol. 20, no. 11, pp. 1496–1504, 2003.
[53] M. A. Shafer, C. A. Fiebrich, D. Arndt, S. E. Fredrickson, and T. W. Hughes, "Quality assurance procedures in the Oklahoma Mesonetwork," *J. Atmos. Ocean. Technol.*, vol. 17, no. 4, pp. 474–494, Apr. 2000.
[54] B. G. Illston, J. B. Basara, D. K. Fischer, R. L. Elliot, C. Fiebrich, K. C. Crawford, K. Humes, and E. Hunt, "Mesoscale monitoring of soil moisture across a statewide network," *J. Atmos. Ocean. Technol.*, vol. 25, no. 2, pp. 167–182, 2008.
[55] J. B. Basara and T. M. Crawford, "Improved installation procedures for deep-layer soil moisture measurements," *J. Atmos. Ocean. Technol.*, vol. 17, no. 6, pp. 879–884, Jun. 2000.
[56] B. G. Illston, J. B. Basara, D. K. Fisher, C. Fiebrich, R. Humes, R. Elliot, K. C. Crawford, and E. Hunt, "Mesoscale monitoring of soil moisture across a statewide network," *J. Atmos. Ocean. Technol.*, vol. 25, no. 2, pp. 167–182, Feb. 2008.
[57] L. M. Arya and J. F. Paris, "A physicoempirical model to predict the soil moisture characteristic from particle-size distribution and bulk density data," *Soil Sci. Soc. Amer. J.*, vol. 45, no. 6, pp. 1023–1030, 1981.
[58] B. G. Illston, J. B. Basara, and K. C. Crawford, "Seasonal to interannual variations of soil moisture measured in Oklahoma," *Int. J. Climatol.*, vol. 24, no. 15, pp. 1883–1896, Dec. 2004.
[59] K. Scipal, W. Wagner, M. Trommler, and K. Naumann, "The global soil moisture archive 1992–2000 from ERS scatterometer data: First results," in *Proc. IGARSS*, 2002, pp. 1399–1401.
[60] P. A. Dirmeyer, Z. C. Guo, and X. Gao, "Comparison, validation, and transferability of eight multiyear global soil wetness products," *J. Hydrometeorol.*, vol. 5, no. 6, pp. 1011–1033, Dec. 2004.
[61] W. W. Verstraeten, F. Veroustraete, C. J. van der Sande, I. Grootaers, and J. Feyen, "Soil moisture retrieval using thermal inertia determined with visible and thermal spaceborne data, validated for European forests," *Remote Sens. Environ.*, vol. 101, no. 3, pp. 299–314, 2006.
[62] A. Ceballos, K. Scipal, W. Wagner, and J. Martínez-Fernández, "Validation of ERS scatterometer-derived soil moisture data in the central part of the Duero Basin, Spain," *Hydrol. Process.*, vol. 19, no. 8, pp. 1549–1566, May 2005.
[63] T. Pellarin, J.-C. Calvet, and W. Wagner, "Evaluation of ERS scatterometer soil moisture products over a half-degree region in southwestern France," *Geophys. Res. Lett.*, vol. 33, no. 17, p. L17 401, Sep. 2006.
[64] K. Scipal, C. Scheffler, and W. Wagner, "Soil moisture-runoff relation at the catchment scale as observed with coarse resolution microwave remote sensing," *Hydrol. Earth Syst. Sci.*, vol. 9, no. 3, pp. 173–183, Aug. 2005.
[65] J. Parajka, V. Naeimi, G. Blöschl, W. Wagner, R. Merz, and K. Scipal, "Assimilating scatterometer soil moisture data into conceptual hydrologic models at the regional scale," *Hydrol. Earth Syst. Sci.*, vol. 10, no. 3, pp. 353–368, 2006.
[66] D. Zhao, B. Su, and M. Zhao, "Soil moisture retrieval from satellite images and its application to heavy rainfall simulation in eastern China," *Adv. Atmos. Sci.*, vol. 23, no. 2, pp. 299–316, Mar. 2006.
[67] B. Fontaine, S. Louvet, and P. Roucou, "Fluctuations in annual cycles and inter-seasonal memory in West Africa: Rainfall, soil moisture and heat fluxes," *Theor. Appl. Climatol.*, vol. 88, no. 1/2, pp. 57–70, Jan. 2007.
[68] D. Zhao, C. Künzer, C. Fu, and W. Wagner, "Evaluation of the ERS scatterometer-derived soil water index to monitor water availability and precipitation distribution at three different scales in China," *J. Hydrometeorol.*, vol. 9, no. 3, pp. 549–561, 2008.
[69] D. W. Gerten, W. Lucht, S. Schaphoff, W. Cramer, T. Hickler, and W. Wagner, "Hydrologic resilience of the terrestrial biosphere," *Geophys. Res. Lett.*, vol. 32, no. 21, p. L21 408, Nov. 2005.
[70] A. de Wit and C. van Diepen, "Crop model data assimilation with the ensemble Kalman filter for improving regional crop yield forecasts," *Agric. For. Meteorol.*, vol. 146, no. 1/2, pp. 38–56, Sep. 2007.
[71] E. Meier, U. Frei, and D. Nüesch, "Precise terrain corrected geocoded images," in *SAR Processing: Data And Systems*, G. Schreier, Ed. Karlsruhe, Germany: Wichmann, 1993, pp. 173–185.
[72] D. Small, F. Holecz, E. Meier, and D. Nüesch, "Absolute radiometric correction in rugged terrain: A plea for integrated radar brightness," in *Proc. IGARSS*, Seattle, WA, 1998, pp. 330–332.
[73] F. T. Ulaby, B. Moore, and A. K. Fung, *Microwave Remote Sensing—Active and Passive, Vol. II: Radar Remote Sensing and Surface Scattering and Emission Theory*. Norwood, MA: Artech House, 1982.
[74] E. Mougin, A. Lopes, P. L. Frison, and C. Proisy, "Preliminary analysis of ERS-1 wind scatterometer data over land surfaces," *Int. J. Remote Sens.*, vol. 16, no. 2, pp. 391–398, Jan. 1995.
[75] P.-L. Frison and E. Mougin, "Use of ERS-1 wind scatterometer data over land surfaces," *IEEE Trans. Geosci. Remote Sens.*, vol. 34, no. 2, pp. 550–560, Mar. 1996.
[76] D. G. Long, P. J. Hardin, and P. T. Whiting, "Resolution enhancement of spaceborne scatterometer data," *IEEE Trans. Geosci. Remote Sens.*, vol. 31, no. 3, pp. 700–714, May 1993.
[77] Y. Gauthier, M. Bernier, and J.-P. Fortin, "Aspect and incidence angle sensitivity in ERS-1 SAR data," *Int. J. Remote Sens.*, vol. 19, no. 10, pp. 2001–2006, Jul. 1998.
[78] M. P. Mäkynen, T. Manninen, M. H. Similä, J. A. Karvonen, and M. T. Hallikainen, "Incidence angle dependence of the statistical properties of C-band HH-polarization backscattering signatures of the Baltic sea ice," *IEEE Trans. Geosci. Remote Sens.*, vol. 40, no. 12, pp. 2593–2609, Dec. 2002.
[79] W. Wagner, C. Pathe, M. Doubkova, D. Sabel, A. Bartsch, S. Hasenauer, G. Blöschl, K. Scipal, J. Martinez-Fernandez, and A. Löw, "Temporal stability of soil moisture and radar backscatter observed by the advanced synthetic aperture radar (ASAR)," *Sensors*, vol. 8, pp. 1174–1197, 2008.
[80] M. Drusch, E. Wood, H. Gao, and A. Thiele, "Soil moisture retrieval during the Southern Great Plains Hydrology Experiment 1999: A comparison between experimental remote sensing data and operational products," *Water Resour. Res.*, vol. 40, p. W02 504, 2004. DOI: 10.1029/2003WR002441.
[81] M. Drusch, E. Wood, and H. Gao, "Observation operators for the direct assimilation of TRMM microwave imager retrieved soil moisture," *Geophys. Res. Lett.*, vol. 32, no. 15, p. L15 403, Aug. 2005.
[82] W. Wagner, C. Pathe, D. Sabel, A. Bartsch, C. Künzer, and K. Scipal, "Experimental 1 km soil moisture products from ENVISAT ASAR for Southern Africa," in *Proc. ENVISAT Symp.*, Montreux, Switzerland, 2007.
[83] A. Bartsch, K. Scipal, P. Wolski, C. Pathe, D. Sabel, and W. Wagner, "Microwave remote sensing of hydrology in Southern Africa," in *Proc. 2nd Göttingen GIS Remote Sens. Days: Global Change Issues Develop. Emerg. Countries, 4-6 October 2006*, 2006, pp. 269–277.

Carsten Pathe received the Dipl.Geogr. degree from the Friedrich Schiller University of Jena, Jena, Germany, in 2002. He is currently working toward the Ph.D. degree in the Insitute of Photogrammetry and Remote Sensing, Vienna University of Technology, Vienna, Austria, where he has been a Research Project Assistant since 2002 and is working on soil moisture retrieval from Envisat ScanSAR data.

His main scientific interests are the development and application of methods for retrieving geophysical variables over land from active remote sensing data with a particular interest in soil moisture retrieval.

Wolfgang Wagner (M'98–SM'07) was born in Wels, Austria, in 1969. He received the Dipl.Ing. (M.Sc.) degree in physics and the D.Tech. (Ph.D.) degree in remote sensing, both with excellence, from the Vienna University of Technology (TU Wien), Vienna, Austria, in 1995 and 1999, respectively.

In support of his M.S. and Ph.D. studies, he received fellowships to carry research at the University of Berne, Berne, Switzerland; Atmospheric Environment Service Canada; NASA Goddard Space Flight Center; European Space Agency; and the Joint Research Center of the European Commission. From 1999 to 2001, he was with the German Aerospace Agency (DLR). Since 2001, he has been a Professor for remote sensing with the Institute of Photogrammetry and Remote Sensing, TU Wien, where he has been the Head since 2006. His main research interests are geophysical parameter retrieval techniques from remote sensing data and application development. He focuses on active remote sensing techniques, particularly scatterometry, SAR, and airborne laser scanning.

Prof. Wagner has been a member of the Science Advisory Groups for Soil Moisture and Ocean Salinity [European Space Agency (ESA)] and Meteorological Operational satellite program Advanced SCATterometer (European Organization for the Exploitation of Meteorological Satellites and ESA). He was the Committee Chair of the European Geosciences Union Hydrologic Sciences Subdivision on Remote Sensing and Data Assimilation from 2005 to 2008. In the period 2008 to 2012, he will serve as the President of the International Society for Photogrammetry and Remote Sensing Commission VII (Thematic Processing, Modeling and Analysis of Remotely Sensed Data).

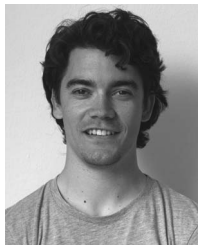

Daniel Sabel was born in Hammarby, Sweden, in 1980. He received the M.Sc. degree in space engineering, with specialization toward remote sensing, from Luleå University of Technology, Luleå, Sweden, in 2007.

Since 2006, he has been with the Institute of Photogrammetry and Remote Sensing, Vienna University of Technology, Vienna, Austria, as a Project Assistant and since 2007 as a University Assistant. His main interests are automated global-scale multitemporal data processing and research in soil moisture retrieval and scaling issues from SAR and scatterometer data.

Marcela Doubkova was born in the Czech Republic in 1980. She studied geography at Charles University, Prague, Czech Republic, in 2000–2003 and at the University of Nebraska, Lincoln, in 2003–2006. She received the M.S. degree in geography from the University of Nebraska in 2006. In her M.S. thesis, she investigated the vegetation and soil water interactions with the use of microwave and optical data.

Since April 2007, she has been a Radar and Geographic Information System Analyst with the Institute of Photogrammetry and Remote Sensing, Vienna University of Technology, Vienna, Austria. Her main research interest encompasses the study of water in soil and vegetation by use of microwave remote sensing and investigation of downscaling techniques for coarse-resolution data.

Jeffrey B. Basara received the B.S. degree in atmospheric science from Purdue University, West Lafayette, IN, and the M.S. and Ph.D. degrees in meteorology from The University of Oklahoma, Norman.

He is currently the Director of Research for the Oklahoma Climatological Survey, The University of Oklahoma. A key component of his research involves the use of the Oklahoma MESONET to gain new insights into processes within the land–atmosphere continuum and how those processes impact complex environmental relationships at varying spatial and temporal scales.